Author Manuscript

Author Manuscript

Author Manuscript

Author Manuscript

HHS Public Access

Author manuscript

Neuron. Author manuscript; available in PMC 2017 January 20.

Published in final edited form as:

Neuron. 2016 January 20; 89(2): 325–336. doi:10.1016/j.neuron.2015.12.024.

A Two-Immunoglobulin-Domain Transmembrane Protein Mediates an Epidermal-Neuronal Interaction to Maintain Synapse Density

Salvatore J. Cherra III[1] and **Yishi Jin**[1,2,3,*]

[1]Division of Biological Sciences, Section of Neurobiology, University of California, San Diego, La Jolla, CA 92093, USA.

[2]Department of Cellular and Molecular Medicine, University of California, San Diego, La Jolla, CA 92093, USA.

[3]Howard Hughes Medical Institute, University of California, San Diego, La Jolla, CA 92093, USA.

Summary

Synaptic maintenance is essential for neural circuit function. In the *C. elegans* locomotor circuit, motor neurons are in direct contact with the epidermis. Here, we reveal a novel epidermal-neuronal interaction mediated by a two-immunoglobulin domain transmembrane protein, ZIG-10, that is necessary for maintaining cholinergic synapse density. ZIG-10 is localized at the cell surface of epidermis and cholinergic motor neurons, with high levels at areas adjacent to synapses. Loss of *zig-10* increases the number of cholinergic excitatory synapses and exacerbates convulsion behavior in a seizure model. Mis-expression of *zig-10* in GABAergic inhibitory neurons reduces GABAergic synapse number, dependent on the presence of ZIG-10 in the epidermis. Furthermore, ZIG-10 interacts with the tyrosine kinase SRC-2 to regulate the phagocytic activity of the epidermis to restrict cholinergic synapse number. Our studies demonstrate the highly specific roles of non-neuronal cells in modulating neural circuit function, through neuron-type specific maintenance of synapse density.

Keywords

synapse maintenance; excitation inhibition balance; non-neuronal cells; locomotion; *C. elegans*

[*]**Contact:** Correspondence to: yijin@ucsd.edu.

Publisher's Disclaimer: This is a PDF file of an unedited manuscript that has been accepted for publication. As a service to our customers we are providing this early version of the manuscript. The manuscript will undergo copyediting, typesetting, and review of the resulting proof before it is published in its final citable form. Please note that during the production process errors may be discovered which could affect the content, and all legal disclaimers that apply to the journal pertain.

Author Contributions

S. J. C. and Y. J. conceived and designed the study. S. J. C. performed all experiments. S. J. C. and Y. J. analyzed the data and wrote the manuscript.

Author Manuscript Author Manuscript Author Manuscript Author Manuscript

Introduction

Maintenance of synaptic connections throughout the lifetime of an organism is important for learning, memory, decision-making, and adaptive behavioral outputs. Synaptic connectivity is regulated not only by neurons, but also by adjacent non-neuronal cells. Glial cells enhance synaptogenesis to guide the formation of discrete circuits in the developing nervous system (Colon-Ramos, 2009; Corty and Freeman, 2013). Astrocytes and microglia modulate synapse formation through many secreted factors, such as hevin, thrombospondins, BDNF, TNFα, and glypican (Bessis et al., 2007; Clarke and Barres, 2013; Stellwagen and Malenka, 2006). Direct contact between glial cells and axons, partly mediated by protocadherins, integrins, and nectins, is also required for efficient synapse formation (Garrett and Weiner, 2009; Hama et al., 2004; Togashi et al., 2009). Conversely, glial cells can reduce synapse density through various mechanisms. Astrocytic secretion of SPARC opposes synapse formation by antagonizing hevin-enhanced synaptogenesis (Kucukdereli et al., 2011). Furthermore, microglia and astrocytes directly eliminate excitatory and inhibitory synapses through distinct phagocytic programs using the complement cascade or MEGF10, respectively (Chung et al., 2013; Schafer et al., 2012). These functions of non-neuronal cells contribute to achieving an optimal level of excitatory and inhibitory synapses that is essential for circuit function; deviation from an excitation and inhibition balance has been associated with neurological disorders (Lisman, 2012; Rubenstein, 2010; Stafstrom, 2006). While many types of interactions between neurons and non-neuronal cells can modulate synaptic connectivity, a gap in our knowledge remains to be how neuron-specific synapse maintenance is achieved at the molecular level.

The immunoglobulin (Ig) domain superfamily (IgSF) is a large, well-conserved family of proteins that regulates many aspects of neural circuit formation, including neurite outgrowth, target identification, and synaptogenesis. Secreted and transmembrane IgSF proteins guide axons and dendrites to precise target areas for synapse formation (Aurelio et al., 2002; Dickson and Gilestro, 2006; Zipursky and Grueber, 2013). Once pre- and post-synaptic compartments arrive at their target areas, distinct members of IgSF subfamilies, such as Sidekicks and Dscams, specify synaptic connections between neurons in discrete laminae of the retina (Millard et al., 2010; Yamagata and Sanes, 2008; Yamagata et al., 2002). Additional homophilic and heterophilic interactions between pre-and post-synaptic IgSF molecules, such as SynCAM, NCAM, and nectins, further assist in the formation of synapses (Togashi et al., 2009). In the mouse cortex the L1CAM family of proteins expressed in glial cells facilitate inhibitory synapse formation (Ango et al., 2008). To date many cell adhesion molecules, including members of the IgSF have been identified as intrinsic factors for synapse formation and specification; however far less is known regarding the roles of IgSF proteins expressed in non-neuronal cells.

C. elegans has a simple nervous system and a small number of non-neuronal cells. Previous studies have shown that expression of the IgSF member, SYG-2/Nephrin in the vulval epidermis specifies synapse location of HSN neurons (Shen et al., 2004). More recently, FGFR expressed in epidermal cells has been shown to regulate glial morphology and in turn synapse location (Shao et al., 2013).

Author Manuscript Author Manuscript Author Manuscript Author Manuscript

Here, we use *C. elegans* as a model to investigate how the interactions between non-neuronal cells and neurons regulate synapse maintenance. In the locomotor circuit two types of motor neurons form synapses onto body wall muscles and provide cholinergic excitation and GABAergic inhibition that underlie sinusoidal locomotion (Richmond and Jorgensen, 1999; White et al., 1976). A sheath of epidermal tissue encompasses the nervous system and makes close contact with neuromuscular junctions (NMJs) (White et al., 1986). We have previously shown that a gain of function (gf) mutation in a cholinergically expressed acetylcholine receptor subunit (ACR-2) perturbs the excitation and inhibition balance of the locomotor circuit, resulting in spontaneous convulsions, a genetic model mimicking seizure (Jospin et al., 2009; Stawicki et al., 2011; Zhou et al., 2013). Interestingly, the convulsion behavior in *acr-2(gf)* animals can be modulated by ion transport in the epidermis (Stawicki et al., 2011), indicating that the epidermis regulates the function of the locomotor circuit.

In this study, we have identified the novel two-Ig-domain IgSF member, ZIG-10, as required for a neuronal-epidermal interaction that continuously maintains the density of excitatory synapses. In the epidermis, ZIG-10 signals through SRC-2 kinase and CED-1 to regulate phagocytic activity. ZIG-10, by controlling cholinergic synapse density, modulates excitation and inhibition balance of the locomotor circuit. Other organisms contain large families of ZIG-10-like proteins, many of which are expressed in neurons and/or glia but whose functions remain mostly unexplored. Our studies reveal the importance of non-neural cells in controlling neuron-type specific synapse maintenance.

Results

An Epidermal RNAi Screen Identifies *zig-10* as a Regulator of Neuromuscular Junctions

To identify genes that function in the epidermis to regulate the locomotor circuit, we designed an RNAi screen in an RNAi-deficient *rde-1(lf); acr-2(gf)* mutant background, in which wild type RDE-1 is expressed in the adult epidermis to restore sensitivity to RNAi solely in the epidermis (Figure 1A, B). *acr-2(gf)* animals are uncoordinated and exhibit an average of 6–8 spontaneous convulsions per minute (Jospin et al., 2009). We reasoned that knockdown of genes that modulate the locomotor circuit would modify the convulsion frequency. By screening a select set of RNAi clones that target predicted cell surface molecules (Hutter et al., 2000) (Table S1), we identified *zig-10* (*zwei* (two) immunoglobulin (Ig) domain protein 10), knockdown of which increased the convulsion frequency in *acr-2(gf)* animals (Figure 1C). ZIG-10 is a member of a family of transmembrane proteins that contain only two extracellular Ig domains; other proteins with similar overall topology include the mammalian junctional adhesion molecules (JAMs) and the Drosophila defective probiscus extension response (DPR) proteins (Figure 1D; Figure S1A–S1D) (Rougon and Hobert, 2003). Proteins of this family generally function as homophilic or heterophilic adhesion molecules (Santoso et al., 2005), but can also act as chaperones for plasma membrane transporters or integrins (Kobayashi et al., 2014; Mandell et al., 2005). We tested if ZIG-10 could form homophilic interactions using a HEK293T cell expression system, and found that HA::ZIG-10 and GFP::ZIG-10 could co-immunoprecipitate (Figure 1E). We validated RNAi effects using two *zig-10* genetic mutations: a null (0) mutation *tm6127* and a missense mutation in the first Ig domain, *gk144897* (lf) (Figure 1D; Figure 1F; Figure S1A–

Author Manuscript Author Manuscript Author Manuscript Author Manuscript

S1B; see Experimental Procedures). A null mutation in a closely related gene, *zig-1*, showed no effect on *acr-2(gf)* convulsions (Table S1; data not shown). Moreover, transgenic expression of wild type *zig-10* fully rescued the enhanced effects on convulsion frequency (Figure 1F; Table S2; Table S3).

zig-10 Mutants Display Increased Density of Neuromuscular Junctions

We investigated the localization of ZIG-10 using a GFP::ZIG-10 fusion protein driven by its endogenous promoter (Figure 2A). GFP::ZIG-10, which fully rescued *zig-10(0)* (Figure 1E), was visible from late embryonic stages to adult in a subset of head neurons, cholinergic motor neurons in the nerve cord, and the epidermis, including the seam cells (Figure 2B–2D; Figure S2A). The subcellular pattern of GFP::ZIG-10 was consistent with plasma membrane localization (Figure 2D; Figure S2A). Around the nerve cord, GFP::ZIG-10 displayed a combination of diffuse and punctate localization at the cell surface (Figure 2B–2C). To determine the localization of ZIG-10 relative to cholinergic synapses, we analyzed transgenic animals that expressed mKate2::ZIG-10 under the *zig-10* promoter and UNC-10::GFP in a subset of cholinergic neurons and found that while mKate2::ZIG-10 was more diffuse than UNC-10::GFP, high levels of mKate2::ZIG-10 tended to be adjacent to UNC-10::GFP (Figure 2E–F).

To address if *zig-10* mutants affected synapses, we examined the pattern of endogenous UNC-10/RIM, an active zone protein, by immunostaining (Koushika et al., 2001). In the wild type animals, UNC-10 displayed discrete puncta throughout the nervous system, with frequent gaps (~1.8 μm or larger) of no staining at random positions along the nerve cords (Schaefer et al., 2000) (Figure 3A; Figure S3A). In both *zig-10* mutants, we observed significantly more presynaptic UNC-10 puncta in wild type animals, accompanied with fewer gaps lacking UNC-10 staining (Figure 3A–3C; Figure S3B–S3G). The size and intensity of individual UNC-10 puncta were similar between *zig-10* mutants and wild type (Figure 3D–3E). The ultrastructural organization of *zig-10(0)* synapses appeared normal (Figure S3H–S3I). Expression of GFP::ZIG-10 under its endogenous promoter fully rescued the excessive number of synapses in *zig-10* mutant animals (Figure 3C–3E; Figure S3C–S3E). Thus, the normal function of ZIG-10 is to constrain synapse formation.

ZIG-10 Specifically Constrains Density of Cholinergic Synapses

We next determined if *zig-10(0)* differentially affected the NMJs formed by cholinergic and GABAergic neurons. We analyzed several presynaptic markers driven by motor neuron-specific promoters, including the active zone protein ELKS-1, or the synaptic vesicle proteins RAB-3 and SNB-1/Synaptobrevin (Table S2). *zig-10(0)* animals showed more cholinergic synapses (Figure 4A–4B; Figure 5B), but displayed normal numbers of GABAergic synapses (Figure 4C–4D; Figure S4A–S4B). Moreover, *zig-10(0)* animals showed an increase in both levamisole-sensitive (UNC-63-containing) and nicotine-sensitive (ACR-16-containing) acetylcholine receptors expressed in the muscle (Figure 4E–4F; Figure S4C–S4D). The increase of acetylcholine receptors correlated with a hypersensitivity to levamisole (Figure S4E), an agonist for UNC-63-containing acetylcholine receptors (Brenner, 1974; Lewis et al., 1980). In contrast, we detected no noticeable differences for the muscle GABA receptor UNC-49 (Figure 4F–4G). The increase in cholinergic synapse

Author Manuscript Author Manuscript Author Manuscript Author Manuscript

number correlated with the enhanced convulsions of *zig-10(0); acr-2(gf)* animals. Although *acr-2(gf)* animals displayed increased cholinergic activity, the number of NMJs was normal (Figure 3F) (Jospin et al., 2009). *zig-10(0); acr-2(gf)* animals displayed an increase in synapses similar to *zig-10(0)* animals (Figure 3F), suggesting that the increased cholinergic synapses caused further imbalance between excitation and inhibition. Together, these data show that *zig-10* specifically limits the number of cholinergic NMJs.

Epidermal and Cholinergic ZIG-10 is Required for Synapse Maintenance

To address in which tissues *zig-10* acts, we transgenically expressed ZIG-10 in specific tissues both in the *zig-10(0); acr-2(gf)* background, assaying convulsion behavior for a functional readout and in *zig-10(0)* animals assaying anatomical effect by synapse number. Transgenic overexpression of GFP::ZIG-10 under its endogenous promoter was sufficient to reduce the convulsion frequency of *zig-10(0); acr-2(gf)* to *acr-2(gf)* single mutant levels (Figure 5A). Overexpression of ZIG-10 in *acr-2(gf)* alone or in wild type background did not cause detectable locomotion phenotypes (Figure 5A; data not shown). Expression of GFP::ZIG-10 in either cholinergic motor neurons (*Punc-17β*), adult epidermis (*Pcol-19*), or muscle (*Pmyo-3*) did not show any rescuing activity (Figure 5A). Simultaneous expression of GFP::ZIG-10 in both the epidermis and cholinergic motor neurons, however, was sufficient to fully rescue the behavioral effects of *zig-10(0)*. In contrast, simultaneous expression of ZIG-10 in both the muscle and cholinergic motor neurons or in both the muscle and epidermis failed to rescue (Figure 5A). Consistent with the functional outcome, the increased synapse number in *zig-10(0)* adult animals was reduced to wild type levels only when ZIG-10 was expressed simultaneously in cholinergic motor neurons and the epidermis, but not when ZIG-10 was expressed in either tissue alone (Figure 5B). Furthermore, simultaneous expression of ZIG-10 in cholinergic motor neurons and in the epidermis fully rescued the increased UNC-63::YFP expression in *zig-10(0)* animals, suggesting that ZIG-10 may influence the levels of postsynaptic acetylcholine receptors indirectly through its function in regulating presynaptic or epidermal compartments (Figure 5C). To address whether the expression of ZIG-10 in the epidermis or cholinergic neurons could be dependent on each other, we analyzed the localization of GFP::ZIG-10 expressed in cholinergic neurons or the epidermis in wild type and *zig-10(0)* animals. We observed that epidermal ZIG-10 localization near synapses marked by UNC-10 was significantly reduced in *zig-10(0)* compared to wild type (Figure S4F). Conversely, neuronal ZIG-10 localization near synapses showed a slight decrease when ZIG-10 was absent in epidermis; however, this mild effect did not reach statistical significance (Figure S4F). Additionally, epidermal ZIG-10 expression in *zig-10(lf)*, which contains an amino acid substitution in the Ig1 domain, did not rescue the convulsion phenotype (Figure S4G). Thus, the requirement for ZIG-10 co-expression in epidermis and neurons suggests that ZIG-10 could act as a homophilic molecule, and that its function involves the first Ig domain.

ZIG-10 Functions Continuously throughout Development and Adult

zig-10(0); acr-2(gf) animals displayed an enhanced convulsion frequency from larvae to adults (Figure S5A). ZIG-10 driven by the *col-19* promoter was only expressed during and after late larval (L4) molting into adult and persisted into at least three day old adults (Figure S5C; data not shown). In the presence of cholinergic ZIG-10, *Pcol-19-GFP::ZIG-10* showed

Author Manuscript Author Manuscript Author Manuscript Author Manuscript

rescue of the synaptic phenotype in *zig-10(0)* from day 1 to day 3 adults (Figure S5E–S5F). However, we observed that larval (L3) *zig-10(0)* animals that co-expressed ZIG-10 in the epidermis (*Pcol-19*) and in cholinergic motor neurons (*Punc-17β*) did not show rescue of the synapse phenotype (Figure S5E–S5F). To further test whether ZIG-10 is required continuously for synapse maintenance during development, we co-expressed ZIG-10 in cholinergic motor neurons using *Punc-17β* and larval epidermis using *Pdpy-7*, which is active in embryonic and larval epidermis but not in adult epidermis (Figure S5B). We observed that this expression was sufficient to restore synapses to wild type levels in larval *zig-10(0)* animals but not in adults (Figure S5E–S5F). Interestingly, GFP::ZIG-10 expressed in larval epidermis was rapidly diminished by the onset of adulthood, compared to free GFP (Figure S5D), suggesting that ZIG-10 protein might undergo rapid degradation. Together, these data show that ZIG-10 is required continuously to maintain synapse number in developing and adult animals.

Ectopic ZIG-10 in GABAergic Neurons Decreases Synapse Number

ZIG-10 is not expressed in GABAergic motor neurons (Figure S2G), which also closely associate with the epidermis and form synapses onto the same muscles as the cholinergic neurons (White et al., 1976). To determine if ZIG-10 is sufficient to modulate GABAergic synapse density, we ectopically expressed ZIG-10 in GABAergic neurons (*Punc-25*, designated P_{GABA}*-ZIG-10*). In a wild type background, we observed a reduction in GABAergic synapse number and increase in UNC-10 negative gaps (Figure 6A–6B; Figure S6A–S6B). This ectopic expression of P_{GABA}-ZIG-10 also caused a significant increase in convulsion frequency in *acr-2(gf)* (Figure 6C). However, in *zig-10(0)* animals P_{GABA}-ZIG-10 expression did not alter GABAergic synapse density, nor did it affect the convulsion frequency of *zig-10(0); acr-2(gf)* (Figure 6B–6C). Moreover, in *zig-10(0); acr-2(gf)* animals, ectopic expression of ZIG-10 in both GABAergic neurons and in the epidermis (P_{GABA}*-ZIG-10+Pcol-19-ZIG-10*) caused a further increase in convulsion frequency (Figure 6C). These results demonstrate that ZIG-10 is sufficient to prevent synapse formation, and further support our conclusion that ZIG-10 mediates an epidermal-neuronal homophilic interaction.

SRC-2 Kinase Functions Downstream of ZIG-10

To determine how ZIG-10 functions, we analyzed two ZIG-10 truncation mutants: ZIG-10-ΔICD, which removes the entire intracellular domain (45 amino acids) and ZIG-10-ΔTM-ICD, which removes both the transmembrane and intracellular domains (Figure S7A). Expression of ZIG-10-ΔICD or ZIG-10-ΔTM-ICD under its endogenous promoter in *zig-10(0); acr-2(gf)* did not rescue the enhanced convulsions (Figure S7B). We also expressed ZIG-10-ΔICD differentially in epidermis or neurons while providing wild type ZIG-10 in the neuron or epidermis, respectively. Regardless of which cells expressed ZIG-10-ΔICD, neither combination was sufficient to provide full function of ZIG-10 (Figure S7B). These results suggest that ZIG-10 function depends on its intracellular domain to mediate signaling in both the epidermis and neurons.

We identified several predicted SH3 ligand motifs in the ZIG-10 intracellular domain (Figure 1D; Figure S1D). We next searched for genes encoding SH3-containing proteins that might be required for ZIG-10 function by taking advantage of the enhanced convulsion

Author Manuscript Author Manuscript Author Manuscript Author Manuscript

frequency of adult animals of *zig-10(0); acr-2(gf); Ex[P_{GABA}-ZIG-10+Pcol-19-ZIG-10]* (Figure 6C; Figure 7A; Table S2; Table S4). We reasoned that knockdown of such genes should reduce the convulsion frequency in these animals. The top hit identified in this screen was SRC-2, a Src family kinase (Table S4). We validated the RNAi effect using a *src-2(0)* null mutation (Figure 7B). *src-2(0)* single mutants had no obvious locomotor phenotype, but *src-2(0); acr-2(gf)* animals showed a significant increase in convulsion frequency, which was not further enhanced in *src-2(0); zig-10(0); acr-2(gf)* triple mutants (Figure 7C), suggesting that ZIG-10 and SRC-2 are in the same pathway. Moreover, using heterologous expression in HEK293T cells, we found that ZIG-10 and SRC-2 formed a complex as observed by co-immunoprecipitation (Figure 7D). Thus SRC-2 interacts with ZIG-10 and functions downstream of ZIG-10. Since *C. elegans* neurons are generally refractory to RNAi (Kamath et al., 2001; Tavernarakis et al., 2000) and we were able to observe effects of *src-2*(RNAi) in a non-sensitized background, *src-2* most likely functions in non-neuronal cells.

The Phagocytosis Pathway Functions Together with SRC-2 to Constrain Synapse Density

Src kinases have been implicated in many pathways that modulate cell proliferation (Roche et al., 1995), cell morphology (Yeatman, 2004), and phagocytosis (Ziegenfuss et al., 2008). In *Drosophila*, Src42A has been shown to regulate phagocytic activity of glial cells during axonal degeneration by phosphorylating the phagocytic receptor Draper (Zhou et al., 2001; Ziegenfuss et al., 2008). The *C. elegans* Draper ortholog CED-1 mediates phagocytosis of cell corpses, and is expressed in the epidermis and motor neurons (Zhou et al., 2001). Similar to *src-2(0); acr-2(gf)* mutants, *ced-1(0); acr-2(gf)* mutants displayed an increase in convulsion frequency, which was not further enhanced in *ced-1(0); zig-10(0); acr-2(gf)* animals (Figure 7C). Importantly, epidermal, but not cholinergic, expression of CED-1::GFP completely rescued the *ced-1(0); acr-2(gf)* phenotype (Figure 8A). To address whether phosphorylation of CED-1 was required for CED-1 function, we expressed a mutant CED-1::GFP, in which tyrosine-1019, a conserved Src phosphorylation site, was mutated to phenylalanine (Y1019F) and found that epidermal expression of CED-1::GFP-Y1019F did not rescue the increased convulsion frequency of *ced-1(0); acr-2(gf)* (Figure 8A), suggesting that CED-1 is likely a target of SRC-2.

In our RNAi screen for SH3 containing proteins, we also noticed moderate effects when knocking down *ced-2* and *ced-5* (Table S4), which are components of the phagocytosis pathway known to function in clearing corpses of dying cells (Ellis et al., 1991). We validated this observation using genetic mutations. We found that, similar to *ced-1(0)*, loss of function in *ced-2*, *ced-5*, as well as *ced-10*, suppressed the enhanced convulsion frequency caused by ectopic ZIG-10 (Figure 7B). This analysis supports a conclusion that the phagocytosis pathway functions downstream of ZIG-10.

We next investigated whether CED-1 directly affected synapses. *ced-1(0)* animals produced an increased number of cholinergic synapses (Figure 8B). *ced-1(0); zig-10(0)* animals displayed no further increase in cholinergic synapses as compared to *zig-10(0)* (Figure 8B). Furthermore, the reduction in GABAergic synapses caused by P_{GABA}-ZIG-10 was abolished in *ced-1(0)* animals (Figure 8C). Together these data support a conclusion that the phagocytosis pathway acts downstream of ZIG-10 to regulate synapse density.

Author Manuscript Author Manuscript Author Manuscript Author Manuscript

ZIG-10 Regulates CED-1-mediated Phagocytosis in Epidermis

To determine how *zig-10(0)* altered synapse density, we next investigated where phagocytosis components were localized with regard to synapses. Using *Pced-1–2xFYVE::GFP* (Yu et al., 2008) as a marker of endosomes and phagosomes and mCherry::RAB-3 expressed only in cholinergic neurons, we observed phagosomes were frequently localized close to or overlapping with presynaptic terminals (Figure 8D). Interestingly, *zig-10(0)* animals showed a significant decrease in the number GFP::2xFYVE-labeled phagosomes associated with cholinergic synapses (Figure 8D and 8F).

We observed similar effects on CED-1. In the epidermis around the nerve cords, CED-1::GFP forms puncta and rings (Figure 8E), resembling the CED-1-containing phagosomes in the intestine and gonad (Zhou et al., 2001). In *zig-10(0)* animals the number of CED-1::GFP-labeled phagosomes in nerve cords was greatly reduced, compared to wild type animals (Figure 8D–8F); however there was no change in CED-1::GFP levels (data not shown). Conversely, *ced-1(0)* showed normal GFP::ZIG-10 expression levels and localization (data not shown). Taken together, these findings suggest that ZIG-10 modulates phagocytic activity through SRC-2 and CED-1 in the epidermis to maintain synapse density.

Discussion

Synapse maintenance occurs in many forms to ensure the function of neural circuits. Our results reveal the IgSF member ZIG-10 as playing a highly specific role in maintenance of excitatory synapse number. ZIG-10 mediates an interaction between cholinergic neurons and epidermis, enabling phagocytic engulfment of synapses by the epidermis. SRC-2 interacts with ZIG-10 and functions downstream of ZIG-10 to modulate synapse maintenance through the regulation of CED-1.

Roles of Ig Superfamily in Maintaining Synapses

Members of the IgSF control many aspects of neural development, such as axon outgrowth and guidance, synapse formation, and cellular avoidance (Aurelio et al., 2002; Hummel et al., 2003; Shen et al., 2004; Wang et al., 2002; Yamagata et al., 2003). Most synaptic IgSF proteins contain at least 3 Ig domains proteins, and some have been shown to mediate signaling pathways in both pre- and post-synaptic neurons during synapse formation (Yamagata et al., 2003). Recent studies have shown that some synaptogenic IgSF proteins also regulate synapse maintenance. For example, after synapse formation, SynCAM levels correlate with hippocampal synapse number, and overexpression of SynCAM causes an increased number of synapses that are maintained as long as SynCAM is overexpressed (Robbins et al., 2010). IgSF9 mediates homophilic binding and does not induce synapse formation, yet, knockout mice display a reduction in GABAergic synapses. Interestingly, IgSF9 appears to function solely as an adhesion molecule since removal of its intracellular domain does not alter its function or GABAergic synapse number (Mishra et al., 2014). In *Drosophila*, an L1-type cell adhesion molecule Neuroglian functions in a heterophilic manner in the presynaptic neurons, and binds to Ankyrin through its cytoplasmic tail to modulate the growth and stability of the neuromuscular junctions (Enneking et al., 2013).

Author Manuscript Author Manuscript Author Manuscript Author Manuscript

Here, we have found that ZIG-10, a member of the two-Ig domain transmembrane protein family constrains cholinergic synapses. Unlike other IgSF proteins that promote synapse formation by acting at pre- or post-synaptic sites, ZIG-10 does not mediate a trans-synaptic interaction since combined cholinergic and muscle expression of ZIG-10 failed to rescue *zig-10(0)*. Instead ZIG-10 function requires its simultaneous expression in neurons and the non-synaptic partners, the epidermis. ZIG-10 localizes to cell surface, and high levels of ZIG-10 are present at regions that border the synapses. Since loss of *zig-10* causes an increase in cholinergic NMJ number, ZIG-10 may occlude the interactions between pre-synaptic neurons and post-synaptic muscle.

ZIG-10 Provides Specificity to Phagocytosis of Synapses

In mammals, synapses destined for elimination are degraded through phagocytosis by non-neuronal cells (Chung et al., 2013; Schafer et al., 2012; Stevens et al., 2007). MEGF10, the mammalian homolog of CED-1, functions in astrocytes to eliminate immature excitatory and inhibitory synapses through phagocytosis in developing and mature circuits (Chung et al., 2013). However, it remains unclear whether astrocytes differentially target synapses in a neuron-specific manner and how glial cells discriminate between excitatory and inhibitory synapses.

Here, our data suggest that cell-type specific expression of IgSF transmembrane proteins provides one level of discrimination for excitatory versus inhibitory synapse maintenance. ZIG-10 mediates an interaction between the epidermis and cholinergic neurons to enable the phagocytosis of cholinergic synaptic material by the epidermis while sparing GABAergic synapses. Moreover, we show that the ZIG-10 pathway provides cellular specificity, since mis-expression of ZIG-10 in GABAergic neurons causes a decrease in GABAergic synapse number. One hypothesis is that ZIG-10 in the epidermis could recruit and activate SRC-2, which then would phosphorylate CED-1, in turn enabling phagocytosis. Since CED-1::GFP is still present on membranes near the nerve cords in *zig-10(0)* mutants, it suggests that ZIG-10 and SRC-2 function to regulate the downstream signaling of CED-1 rather than its localization near synapses. Further studies will be required to determine how ZIG-10 activates SRC-2 and how synapses are specified for elimination.

While *C. elegans* has only 2 transmembrane two-Ig domain proteins, vertebrate and Drosophila genomes contain a greatly expanded set of transmembrane two-Ig domain proteins (Figure S1) (Rougon and Hobert, 2003). Emerging evidence suggests that ZIG-10 homologs may also establish specific cellular connections. A recent study has found that the IgSF protein, neurofascin-155 is expressed by mammalian glial cells and regulates cholinergic synapse elimination at the neuromuscular junction (Roche et al., 2014). Similar to ZIG-10, mammalian neurofascin-155, *C. briggsae* ZIG-10 and *Drosophila* DPR-8 also contain predicted SH3 ligand motifs, suggesting a conservation of downstream signaling pathways. Further, we speculate that differential expression of such two-Ig domain proteins may provide cell-type selectivity for how individual circuits retain robustness during development or in response to changes in neuronal activity or even disease.

Author Manuscript Author Manuscript Author Manuscript Author Manuscript

Experimental Procedures

Strains and transgenes

C. elegans strains were maintained at room temperature on nematode growth media (NGM) as previously described (Brenner, 1974), except for RNAi experiments as detailed below. The wild type strain is Bristol N2. All strains and alleles used in this study are described in Table S2; genotypes were confirmed by PCR for deletion alleles, or by sequencing for point mutations and by restriction enzyme digestion. *zig-10(gk144897)* alters an Hpy188III site.

We generated extrachromosomal array transgenic lines as previously described (Mello et al., 1991). We used *Pttx-3-RFP* (80 ng/μl), *Pgcy-8-GFP* (90 ng/μl), or *Pmyo-2-mCherry* (2 ng/μl) as coinjection markers. Expression constructs, transgenes, and strain genotypes are summarized in Tables S2–S3. In general, two independent transgenic lines were observed, and quantitative data shown for one.

RNAi screen

For the epidermal RNAi screen of transmembrane proteins, we used CZ14539 *Pcol-19-RDE-1 (juIs346) III; rde-1(ne219)V* (Xu and Chisholm, 2011) to construct CZ16323 *juIs346[Pcol-10-RDE-1] III; rde-1(ne219) V; acr-2(n2420gf) X*. Animals were synchronized by bleaching gravid adults, and subsequent L1 progeny were placed on NGM plates containing 5 mM IPTG and 25 μg/ml carbenicillin (Sigma) that had been seeded with RNAi-expressing HT115 bacteria (Kamath et al., 2003). Three days later adult animals were assessed by visual inspection for convulsion frequency; 8–10 animals counted per RNAi clone for three biological replicates.

For the RNAi screen of SH3-domain containing proteins, adult animals of *zig-10(0); acr-2(gf); juEx6249[Punc-25-GFP::ZIG-10 +Pcol-19-GFP::ZIG-10]* (CZ20628) were placed on RNAi plates. Their adult progeny were scored visually for convulsion frequency; 8–10 animals were counted per RNAi clone for three biological replicates.

Whole mount immunocytochemistry and image analysis

We followed a standard fixation procedure (Finney and Ruvkun, 1990) with minor modifications (Supplemental Experimental Procedures). All samples were imaged on a Zeiss LSM710 confocal microscope under identical settings. To quantify the number and size of presynaptic puncta labeled by anti-UNC-10/RIM2, images of dorsal cord were analyzed over a 50 μm distance using the Analyze Particles function of NIH ImageJ. Synaptic gaps were defined as asynaptic regions lacking UNC-10 staining that were greater than 2 μm (Schaefer et al., 2000); these UNC-10 negative gaps were manually quantified using the Grid plugin in ImageJ with an area per point setting of 2 μm. Interpunctal distance was calculated using the Analyze Particles function of ImageJ to obtain the centroid mass for each punctum; the distance between puncta was then calculated.

For imaging of SNB-1::GFP, ELKS-1::Cerulean, or RAB-3::CFP, live worms were immobilized with 10 mM levamisole. The number of presynaptic terminals labeled by SNB-1::GFP, ELKS-1::Cerulean, or RAB-3::CFP was manually counted. For analysis of

Author Manuscript Author Manuscript Author Manuscript Author Manuscript

developmental regulation of synapse maintenance, the total number of presynaptic puncta in the axon were manually counted at L3, adult Day 1, and adult Day 3 stages.

To analyze the levamisole-sensitive acetylcholine receptors labeled by UNC-63::YFP(*kr98*) in which YFP was inserted to the endogenous genomic locus of *unc-63* and the GABA receptors labeled by transgenic UNC-49::GFP, L4 animals were placed in M9 on a 10% agarose pad with no anesthetics and were rolled to obtain a dorsal view of the dorsal nerve cord for imaging. Animals expressing *Pmyo-3-ACR-16::GFP* to label levamisole-insensitive acetylcholine receptors were immobilized with 10 mM levamisole and imaged as described. The images were then analyzed using the Analyze Particles function of NIH ImageJ to quantify the fluorescence intensity; all measurements were normalized to the measured area.

For imaging GFP::2xFYVE or CED-1::GFP in the vicinity of the dorsal nerve cord, L4 animals were rolled to image the animals from the dorsal aspect with no anesthetics. Images were captured through the entire depth of the dorsal cord using *Punc-17β-mCherry* as a neuronal marker for the dorsal cord. CED-1::GFP-labeled phagosomes were defined as ring-like structures that encompassed cholinergic neuronal structures visualized by *Punc-17β-mCherry*.

DNA Plasmid construction

Pzig-10-GFP (pCZGY2615) was produced by cloning the 4.3 kb *zig-10* promoter into the destination vector upstream of the attR1-chloramphenicol resistance gene-ccdB gene-attR2 cassette using the Gibson cloning method (Gibson et al., 2009). GFP with introns was then cloned into the *Pzig-10*-destination vector by LR reaction.

Full-length functional *GFP::ZIG-10* (pCZGY2602) was generated by cloning the genomic locus of *zig-10* from the WRM065cF08 fosmid in two pieces: the 4.3 kb *zig-10* 5’ upstream sequences to amino acid 20 of ZIG-10 and amino acid 21 to 890 base pairs 3’ downstream of the stop codon. Restriction enzyme sites were incorporated by PCR allowing for the insertion of monomeric GFP into *zig-10* after amino acid 20. All tissue-specific *zig-10* rescue plasmids were generated using *GFP-ZIG-10* coding sequence cloned into pCR8-GW/TOPO from genomic DNA and subsequently cloned into Gateway destination vectors containing promoters of interest.

A cDNA clone (yk1568) for *zig-10* was kindly provided by Y. Kohara. This clone contains the 5’ splice leader sequence (SL1), the *zig-10* coding sequence, and the 3’ untranslated region and corresponds to the full-length transmembrane domain-containing ZIG-10. The *zig-10* cDNA was cloned into pCR8-GW/TOPO; further cloning was performed using the Gateway system. ZIG-10 truncations (pCZGY2614 and pCZGY2619, respectively) were generated by PCR.

RNA Analysis of *zig-10(tm6127)*

RNA was isolated from mixed stage worms from either wild type or *zig-10(tm6127)* background using Trizol according to manufacturer’s specifications. cDNA was generated using SuperScript First Strand Synthesis kit (Invitrogen). To determine the effect of *zig-10(tm6127)* deletion at the transcript level, RT-PCR was performed using primers (5’-

Author Manuscript Author Manuscript Author Manuscript Author Manuscript

ctgaatgagaggaagccacg-3’ and 5’-aggagctaaccgaggatctg-3’), and the corresponding DNA fragments were analyzed by sequencing. The *zig-10(tm6127)* deletion disrupts exon splicing and results in changes from amino acid 137-YFQKPKKVIIICFHPKHIEFSF-158, followed by premature termination.

Behavioral Analysis

For behavioral analysis late larval (L4) worms were grown overnight at room temperature and transferred to a fresh plate the following day for analysis. For the levamisole sensitivity assay, worms were moved to fresh plates containing levamisole (1 mM in NGM; Sigma). To assess convulsion frequency in worms expressing *acr-2(gf)*, worms were moved to a fresh plate and visually observed for 90 seconds to quantify the convulsion frequency. A convulsion was defined as a visible shortening in length between nose and tail (Jospin et al., 2009; Stawicki et al., 2011).

Cell Culture and Biochemistry

HEK293T cells (ATCC) were grown in DMEM (Cell Gro) supplemented with 10% fetal calf serum (Life Technologies). GFP::ZIG-10, HA::ZIG-10, or HA::SRC-2 were transfected as indicated using Lipofectamine 2000 (Invitrogen) according to manufacturer’s specifications. Two days after transfection the cells were collected in lysis buffer (50 mM Tris-HCl, pH 7.5; 1% Igepal CA-630; 150 mM NaCl). After clearing cellular debris by centrifugation, the lysates were subjected to immunoprecipitation using HA-microbeads (Miltenyi) according to manufacturer’s specifications. The eluate from immunoprecipitation and 50 μg of lysate were separated by SDS-PAGE and transferred to PDVF membranes. Membranes were probed with antibodies against GFP (1:2000, RRID:AB_303395, Abcam), HA (1:1000, RRID:AB_10691311, Cell Signaling), and actin (1:6000, RRID:AB_2336056, MPBio).

Statistical Analysis

All graphical data are presented as mean ± SEM. A two-tailed *t*-test was used to compare data between two groups. All quantitative data involving more than two groups was compared using a one-way ANOVA for parametric data followed by a *post-hoc t*-test with Bonferroni’s correction for multiple comparisons. For non-parametric data, means were compared using a Kruskal-Wallis test followed by Dunn’s multiple comparison tests. $P<0.05$ (*) was considered statistically significant. Power analysis was performed to attain sample sizes that would provide a beta error ≤ 0.2.

Supplementary Material

Refer to Web version on PubMed Central for supplementary material.

Acknowledgments

We thank J.-L. Bessereau, J.S. Dittman, E.M. Jorgensen, J.M. Kaplan, Y. Kohara, A.V. Maricq, K. Shen, and Z. Zhou for strains and reagents. We acknowledge A. Goncharov for electron microscopy and A. D. Chisholm and our lab members for advice and comments. Some strains were provided by S. Mitani and the *Caenorhabditis* Genetics Center, which is funded by NIH Office of Research Infrastructure Programs (P40 OD010440). This work was supported by NIH grants (NS035546 to Y. J. and F32 NS081945 to S. J. C. and T32 NS7220) and the Howard Hughes Medical Institute. Y. J. is an Investigator of the Howard Hughes Medical Institute.

Author Manuscript Author Manuscript Author Manuscript Author Manuscript

References

Ango F, Wu C, Van der Want JJ, Wu P, Schachner M, Huang ZJ. Bergmann glia and the recognition molecule CHL1 organize GABAergic axons and direct innervation of Purkinje cell dendrites. PLoS Biol. 2008; 6:e103. [PubMed: 18447583]

Aurelio O, Hall DH, Hobert O. Immunoglobulin-domain proteins required for maintenance of ventral nerve cord organization. Science. 2002; 295:686–690. [PubMed: 11809975]

Bamber BA, Beg AA, Twyman RE, Jorgensen EM. The *Caenorhabditis elegans unc-49* locus encodes multiple subunits of a heteromultimeric GABA receptor. J Neurosci. 1999; 19:5348–5359. [PubMed: 10377345]

Bessis A, Bechade C, Bernard D, Roumier A. Microglial control of neuronal death and synaptic properties. Glia. 2007; 55:233–238. [PubMed: 17106878]

Brenner S. The genetics of *Caenorhabditis elegans* . Genetics. 1974; 77:71–94. [PubMed: 4366476]

Chung WS, Clarke LE, Wang GX, Stafford BK, Sher A, Chakraborty C, Joung J, Foo LC, Thompson A, Chen C, et al. Astrocytes mediate synapse elimination through MEGF10 and MERTK pathways. Nature. 2013; 504:394–400. [PubMed: 24270812]

Clarke LE, Barres BA. Emerging roles of astrocytes in neural circuit development. Nat Rev Neurosci. 2013; 14:311–321. [PubMed: 23595014]

Colon-Ramos DA. Synapse formation in developing neural circuits. Curr Top Dev Biol. 2009; 87:53–79. [PubMed: 19427516]

Corty MM, Freeman MR. Cell biology in neuroscience: Architects in neural circuit design: glia control neuron numbers and connectivity. J Cell Biol. 2013; 203:395–405. [PubMed: 24217617]

Dickson BJ, Gilestro GF. Regulation of commissural axon pathfinding by slit and its Robo receptors. Annu Rev Cell Dev Biol. 2006; 22:651–675. [PubMed: 17029581]

Dinkel H, Chica C, Via A, Gould CM, Jensen LJ, Gibson TJ, Diella F. Phospho.ELM: a database of phosphorylation sites--update 2011. Nucleic Acids Res. 2011; 39:D261–D267. [PubMed: 21062810]

Ellis RE, Jacobson DM, Horvitz HR. Genes required for the engulfment of cell corpses during programmed cell death in Caenorhabditis elegans. Genetics. 1991; 129:79–94. [PubMed: 1936965]

Enneking EM, Kudumala SR, Moreno E, Stephan R, Boerner J, Godenschwege TA, Pielage J. Transsynaptic coordination of synaptic growth, function, and stability by the L1-type CAM Neuroglian. PLoS Biol. 2013; 11:e1001537. [PubMed: 23610557]

Finney M, Ruvkun G. The *unc-86* gene product couples cell lineage and cell identity in *C. elegans* . Cell. 1990; 63:895–905. [PubMed: 2257628]

Garrett AM, Weiner JA. Control of CNS synapse development by γ-protocadherin-mediated astrocyte-neuron contact. J Neurosci. 2009; 29:11723–11731. [PubMed: 19776259]

Gendrel M, Rapti G, Richmond JE, Bessereau JL. A secreted complement-control-related protein ensures acetylcholine receptor clustering. Nature. 2009; 461:992–996. [PubMed: 19794415]

Gibson DG, Young L, Chuang RY, Venter JC, Hutchison CA 3rd, Smith HO. Enzymatic assembly of DNA molecules up to several hundred kilobases. Nat Methods. 2009; 6:343–345. [PubMed: 19363495]

Hama H, Hara C, Yamaguchi K, Miyawaki A. PKC signaling mediates global enhancement of excitatory synaptogenesis in neurons triggered by local contact with astrocytes. Neuron. 2004; 41:405–415. [PubMed: 14766179]

Hummel T, Vasconcelos ML, Clemens JC, Fishilevich Y, Vosshall LB, Zipursky SL. Axonal targeting of olfactory receptor neurons in *Drosophila* is controlled by Dscam. Neuron. 2003; 37:221–231. [PubMed: 12546818]

Hutter H, Vogel BE, Plenefisch JD, Norris CR, Proenca RB, Spieth J, Guo C, Mastwal S, Zhu X, Scheel J, et al. Conservation and novelty in the evolution of cell adhesion and extracellular matrix genes. Science. 2000; 287:989–994. [PubMed: 10669422]

Author Manuscript Author Manuscript Author Manuscript Author Manuscript

Jospin M, Qi YB, Stawicki TM, Boulin T, Schuske KR, Horvitz HR, Bessereau JL, Jorgensen EM, Jin Y. A neuronal acetylcholine receptor regulates the balance of muscle excitation and inhibition in *Caenorhabditis elegans* . PLoS Biol. 2009; 7:e1000265. [PubMed: 20027209]

Kamath RS, Fraser AG, Dong Y, Poulin G, Durbin R, Gotta M, Kanapin A, Le Bot N, Moreno S, Sohrmann M, et al. Systematic functional analysis of the *Caenorhabditis elegans* genome using RNAi. Nature. 2003; 421:231–237. [PubMed: 12529635]

Kamath RS, Martinez-Campos M, Zipperlen P, Fraser AG, Ahringer J. Effectiveness of specific RNA-mediated interference through ingested double-stranded RNA in *Caenorhabditis elegans* . Genome Biol. 2001; 2 RESEARCH0002.0001-0002.0010.

Kittelmann M, Hegermann J, Goncharov A, Taru H, Ellisman MH, Richmond JE, Jin Y, Eimer S. Liprin-alpha/SYD-2 determines the size of dense projections in presynaptic active zones in C. elegans. J Cell Biol. 2013; 203:849–863. [PubMed: 24322429]

Kobayashi I, Kobayashi-Sun J, Kim AD, Pouget C, Fujita N, Suda T, Traver D. Jam1a–Jam2a interactions regulate haematopoietic stem cell fate through Notch signalling. Nature. 2014; 512:319–323. [PubMed: 25119047]

Koushika SP, Richmond JE, Hadwiger G, Weimer RM, Jorgensen EM, Nonet ML. A post-docking role for active zone protein Rim. Nat Neurosci. 2001; 4:997–1005. [PubMed: 11559854]

Kucukdereli H, Allen NJ, Lee AT, Feng A, Ozlu MI, Conatser LM, Chakraborty C, Workman G, Weaver M, Sage EH, et al. Control of excitatory CNS synaptogenesis by astrocyte-secreted proteins Hevin and SPARC. Proc Natl Acad Sci U S A. 2011; 108:E440–E449. [PubMed: 21788491]

Lewis JA, Wu CH, Berg H, Levine JH. The genetics of levamisole resistance in the nematode *Caenorhabditis elegans* . Genetics. 1980; 95:905–928. [PubMed: 7203008]

Lisman J. Excitation, inhibition, local oscillations, or large-scale loops: what causes the symptoms of schizophrenia? Curr Opin Neurobiol. 2012; 22:537–544. [PubMed: 22079494]

Mandell KJ, Babbin BA, Nusrat A, Parkos CA. Junctional adhesion molecule 1 regulates epithelial cell morphology through effects on beta1 integrins and Rap1 activity. J Biol Chem. 2005; 280:11665–11674. [PubMed: 15677455]

Mello CC, Kramer JM, Stinchcomb D, Ambros V. Efficient gene transfer in *C. elegans*: extrachromosomal maintenance and integration of transforming sequences. EMBO J. 1991; 10:3959–3970. [PubMed: 1935914]

Millard SS, Lu Z, Zipursky SL, Meinertzhagen IA. *Drosophila* dscam proteins regulate postsynaptic specificity at multiple-contact synapses. Neuron. 2010; 67:761–768. [PubMed: 20826308]

Mishra A, Traut MH, Becker L, Klopstock T, Stein V, Klein R. Genetic evidence for the adhesion protein IgSF9/Dasm1 to regulate inhibitory synapse development independent of its intracellular domain. J Neurosci. 2014; 34:4187–4199. [PubMed: 24647940]

Richmond JE, Jorgensen EM. One GABA and two acetylcholine receptors function at the *C. elegans* neuromuscular junction. Nat Neurosci. 1999; 2:791–797. [PubMed: 10461217]

Robbins EM, Krupp AJ, Perez de Arce K, Ghosh AK, Fogel AI, Boucard A, Sudhof TC, Stein V, Biederer T. SynCAM 1 adhesion dynamically regulates synapse number and impacts plasticity and learning. Neuron. 2010; 68:894–906. [PubMed: 21145003]

Roche S, Fumagalli S, Courtneidge SA. Requirement for Src family protein tyrosine kinases in G2 for fibroblast cell division. Science. 1995; 269:1567–1569. [PubMed: 7545311]

Roche SL, Sherman DL, Dissanayake K, Soucy G, Desmazieres A, Lamont DJ, Peles E, Julien JP, Wishart TM, Ribchester RR, et al. Loss of glial neurofascin155 delays developmental synapse elimination at the neuromuscular junction. J Neurosci. 2014; 34:12904–12918. [PubMed: 25232125]

Rougon G, Hobert O. New insights into the diversity and function of neuronal immunoglobulin superfamily molecules. Annu Rev Neurosci. 2003; 26:207–238. [PubMed: 12598678]

Rubenstein JL. Three hypotheses for developmental defects that may underlie some forms of autism spectrum disorder. Curr Opin Neurol. 2010; 23:118–123. [PubMed: 20087182]

Santoso S, Orlova VV, Song K, Sachs UJ, Andrei-Selmer CL, Chavakis T. The homophilic binding of junctional adhesion molecule-C mediates tumor cell-endothelial cell interactions. J Biol Chem. 2005; 280:36326–36333. [PubMed: 16118203]

Author Manuscript Author Manuscript Author Manuscript Author Manuscript

Schaefer AM, Hadwiger GD, Nonet ML. rpm-1, a conserved neuronal gene that regulates targeting and synaptogenesis in C. elegans. Neuron. 2000; 26:345–356. [PubMed: 10839354]

Schafer DP, Lehrman EK, Kautzman AG, Koyama R, Mardinly AR, Yamasaki R, Ransohoff RM, Greenberg ME, Barres BA, Stevens B. Microglia sculpt postnatal neural circuits in an activity and complement-dependent manner. Neuron. 2012; 74:691–705. [PubMed: 22632727]

Shao Z, Watanabe S, Christensen R, Jorgensen EM, Colon-Ramos DA. Synapse location during growth depends on glia location. Cell. 2013; 154:337–350. [PubMed: 23870123]

Shen K, Fetter RD, Bargmann CI. Synaptic specificity is generated by the synaptic guidepost protein SYG-2 and its receptor, SYG-1. Cell. 2004; 116:869–881. [PubMed: 15035988]

Stafstrom CE. Epilepsy: a review of selected clinical syndromes and advances in basic science. J Cereb Blood Flow Metab. 2006; 26:983–1004. [PubMed: 16437061]

Stawicki TM, Zhou K, Yochem J, Chen L, Jin Y. TRPM channels modulate epileptic-like convulsions via systemic ion homeostasis. Curr Biol. 2011; 21:883–888. [PubMed: 21549603]

Stellwagen D, Malenka RC. Synaptic scaling mediated by glial TNF-alpha. Nature. 2006; 440:1054–1059. [PubMed: 16547515]

Stevens B, Allen NJ, Vazquez LE, Howell GR, Christopherson KS, Nouri N, Micheva KD, Mehalow AK, Huberman AD, Stafford B, et al. The classical complement cascade mediates CNS synapse elimination. Cell. 2007; 131:1164–1178. [PubMed: 18083105]

Tavernarakis N, Wang SL, Dorovkov M, Ryazanov A, Driscoll M. Heritable and inducible genetic interference by double-stranded RNA encoded by transgenes. Nat Genet. 2000; 24:180–183. [PubMed: 10655066]

Togashi H, Sakisaka T, Takai Y. Cell adhesion molecules in the central nervous system. Cell Adh Migr. 2009; 3:29–35. [PubMed: 19372758]

Wang J, Zugates CT, Liang IH, Lee CH, Lee T. *Drosophila* Dscam is required for divergent segregation of sister branches and suppresses ectopic bifurcation of axons. Neuron. 2002; 33:559–571. [PubMed: 11856530]

White JG, Southgate E, Thomson JN, Brenner S. The structure of the ventral nerve cord of *Caenorhabditis elegans* . Philos Trans R Soc Lond B Biol Sci. 1976; 275:327–348. [PubMed: 8806]

White JG, Southgate E, Thomson JN, Brenner S. The structure of the nervous system of the nematode *Caenorhabditis elegans* . Philos Trans R Soc Lond B Biol Sci. 1986; 314:1–340. [PubMed: 22462104]

Xu S, Chisholm AD. A Galphaq-Ca(2)(+) signaling pathway promotes actin-mediated epidermal wound closure in *C. elegans* . Curr Biol. 2011; 21:1960–1967. [PubMed: 22100061]

Yamagata M, Sanes JR. Dscam and Sidekick proteins direct lamina-specific synaptic connections in vertebrate retina. Nature. 2008; 451:465–469. [PubMed: 18216854]

Yamagata M, Sanes JR, Weiner JA. Synaptic adhesion molecules. Curr Opin Cell Biol. 2003; 15:621–632. [PubMed: 14519398]

Yamagata M, Weiner JA, Sanes JR. Sidekicks: synaptic adhesion molecules that promote lamina-specific connectivity in the retina. Cell. 2002; 110:649–660. [PubMed: 12230981]

Yeatman TJ. A renaissance for SRC. Nat Rev Cancer. 2004; 4:470–480. [PubMed: 15170449]

Yu X, Lu N, Zhou Z. Phagocytic receptor CED-1 initiates a signaling pathway for degrading engulfed apoptotic cells. PLoS Biol. 2008; 6:e61. [PubMed: 18351800]

Zhou K, Stawicki TM, Goncharov A, Jin Y. Position of UNC-13 in the active zone regulates synaptic vesicle release probability and release kinetics. Elife (Cambridge). 2013; 2:e01180.

Zhou Z, Hartwieg E, Horvitz HR. CED-1 is a transmembrane receptor that mediates cell corpse engulfment in *C. elegans* . Cell. 2001; 104:43–56. [PubMed: 11163239]

Ziegenfuss JS, Biswas R, Avery MA, Hong K, Sheehan AE, Yeung YG, Stanley ER, Freeman MR. Draper-dependent glial phagocytic activity is mediated by Src and Syk family kinase signalling. Nature. 2008; 453:935–939. [PubMed: 18432193]

Zipursky SL, Grueber WB. The molecular basis of self-avoidance. Annu Rev Neurosci. 2013; 36:547–568. [PubMed: 23841842]

Author Manuscript Author Manuscript Author Manuscript Author Manuscript

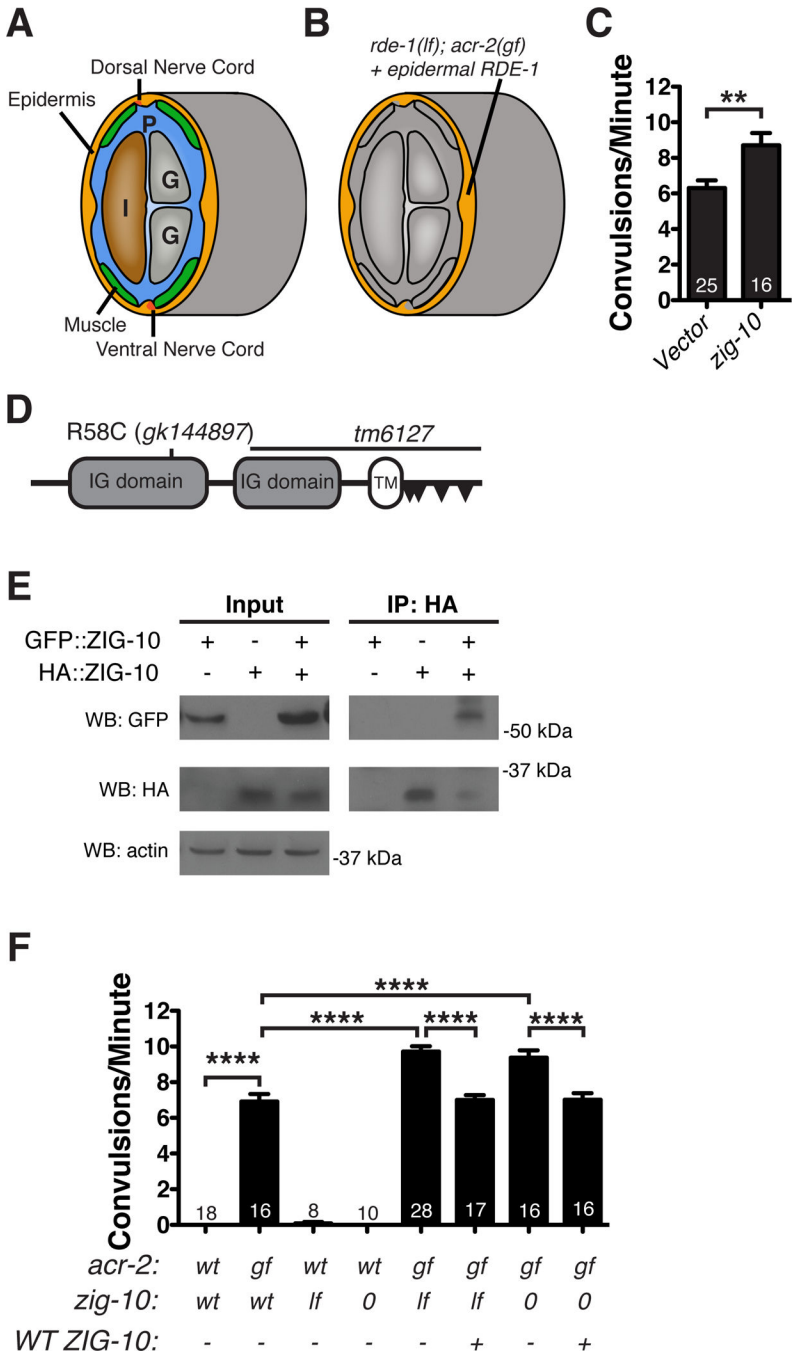

Figure 1. ZIG-10 regulates the locomotor circuit

(**A**) A diagram showing the cross section of a worm to illustrate proximity of the epidermis to the muscle and nerve cords. Other tissues are indicated as intestine, I; gonad, G; the pseudocoelom is indicated as P. (**B**) Epidermal-specific RNAi screen was performed in *juIs346[Pcol-19-RDE-1]; rde-1(lf); acr-2(gf)*, in which RDE-1 was rescued only in adult epidermis (orange), while other tissues remained RNAi defective (gray). (**C**) *zig-10(RNAi)* in *acr-2(gf)* animals increased the frequency of convulsions. (**D**) The predicted ZIG-10 protein consists of 322 aa and contains two extracellular Ig domains, a transmembrane

Author Manuscript Author Manuscript Author Manuscript Author Manuscript

domain, and a short cytoplasmic tail. There is one class II and three non-canonical SH3-ligand motifs indicated by triangles, as predicted by The Eukaryotic Linear Motif resource for Functional Sites in Proteins (Dinkel et al., 2011). (**E**) GFP::ZIG-10 coimmunoprecipitates with HA::ZIG-10 expressed in HEK 293T cells. (**F**) Convulsion frequency analysis in adult animals of genotypes indicated. *zig-10(tm6127)* is indicated as *0; zig-10(gk144897), lf*; + or −, denote presence or absence of *GFP::ZIG-10* driven by its endogenous promoter.

The data in C and F are represented as mean ± SEM. **p≤0.01 and ****p≤0.0001. Sample size is indicated within each bar. See also Figure S1 and Table S1.

Author Manuscript Author Manuscript Author Manuscript Author Manuscript

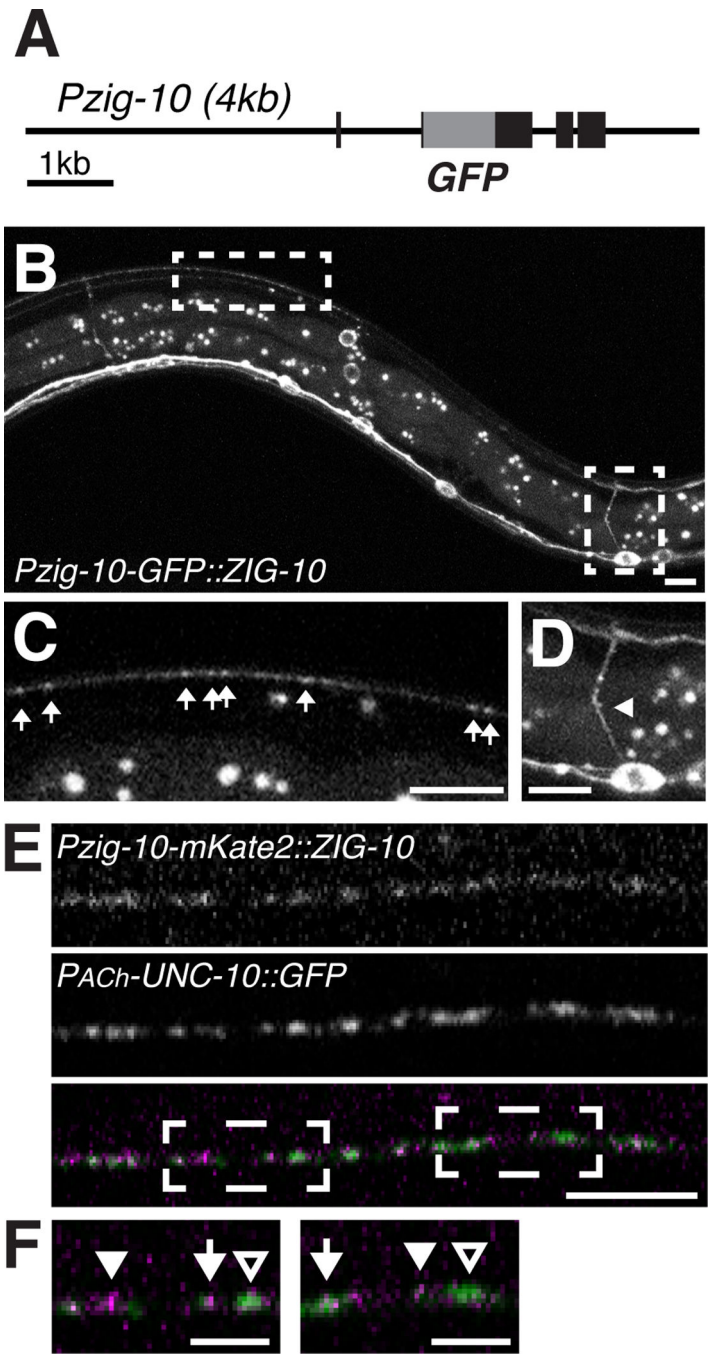

Figure 2. ZIG-10 is expressed in epidermis and cholinergic neurons

(**A**) Diagram of GFP::ZIG-10 fusion protein driven by the *zig-10* endogenous promoter. (**B–D**) Representative images of *GFP::ZIG-10 (juEx5455)* in an L4 transgenic animal, with enlarged views of boxed areas shown in C and D. The puncta between the dorsal and ventral cords are autofluorescent granules in the intestine. Scale bar is 5 μm. (**C**) Punctate GFP::ZIG-10 is visible in the dorsal cord indicated by arrows. (**D**) GFP::ZIG-10 is expressed in the soma and neurite (arrowhead) of motor neurons. (**E**) Confocal 0.5 μm single section of the dorsal cord in animals *coexpressing Punc-129-UNC-10::GFP (nuIs165)* and *Pzig-10-*

Author Manuscript Author Manuscript Author Manuscript Author Manuscript

mKate2::ZIG-10 (juEx7182). Scale bar is 5 μm. (**F**) Enlarged regions of boxed areas in E. Arrows indicate regions where mKate2::ZIG-10 and UNC-10 have similar intensities. Filled arrowheads indicate regions where mKate2::ZIG-10 is higher than UNC-10, and empty arrowheads indicate regions where mKate2::ZIG-10 is lower than UNC-10. Scale bar is 2 μm.

See also Figure S2.

Author Manuscript Author Manuscript Author Manuscript Author Manuscript

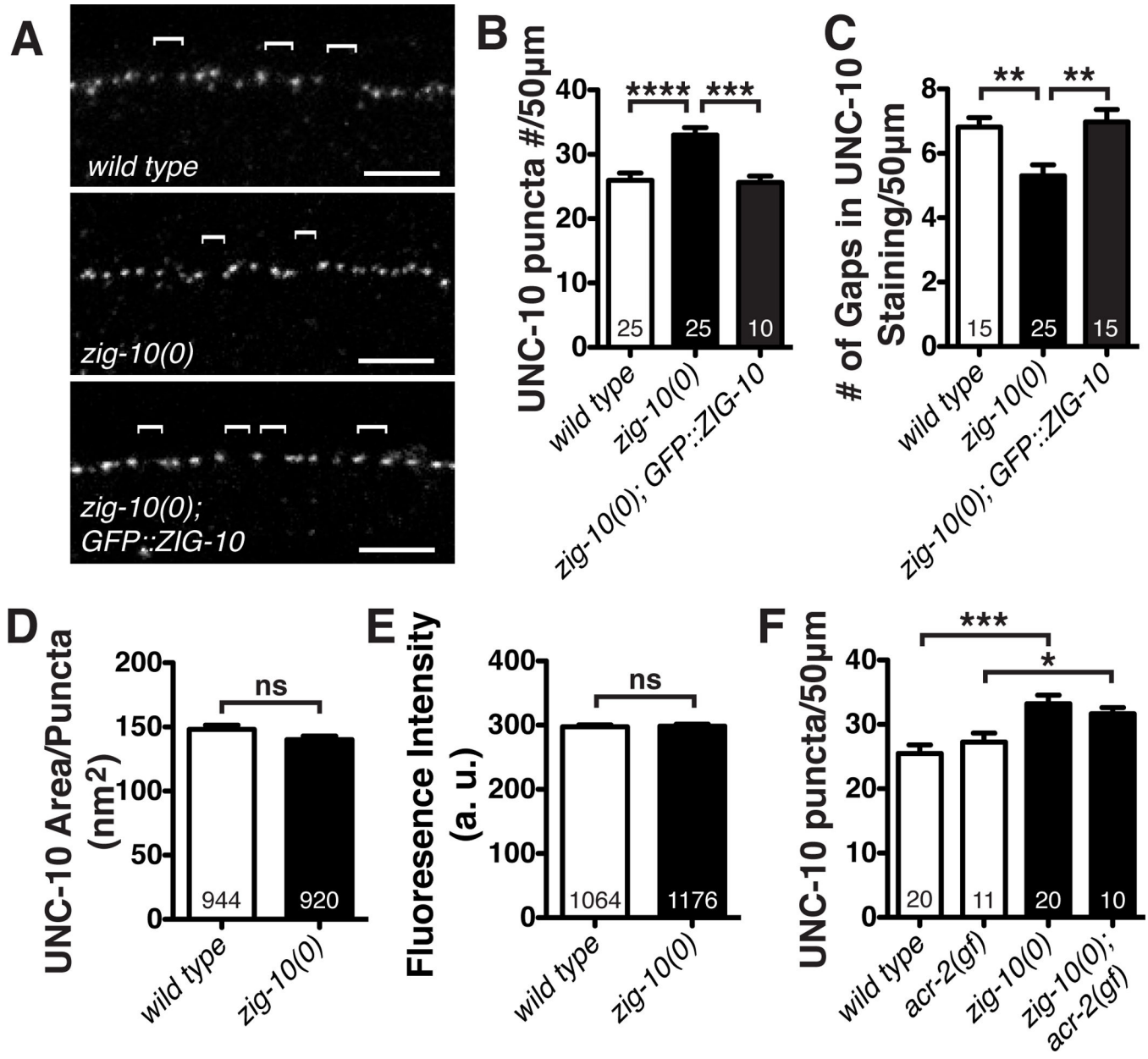

Figure 3. Loss of ZIG-10 increases synapse density

(**A**) Representative confocal images of immunostaining for the active zone protein UNC-10 in the dorsal cord. Brackets mark UNC-10 negative gaps greater than 2 µm. (**B**) *zig-10(0)* displayed an increased number of synapses. (**C**) *zig-10(0)* showed a reduced number of UNC-10 negative gaps between synapses. (**D–E**) *zig-10(0)* had a normal active zone area and did not alter UNC-10 staining intensity as measured in arbitrary units (a. u.). (**F**) *zig-10(0)* increased the number of synapses in *acr-2(gf)* background.

The data in B-F are represented as mean ± SEM. ns=not significant, *p<0.05, **p≤0.01, ***p≤0.001, and ****p≤0.0001. Sample size is shown within each bar. See also Figure S3.

Author Manuscript Author Manuscript Author Manuscript Author Manuscript

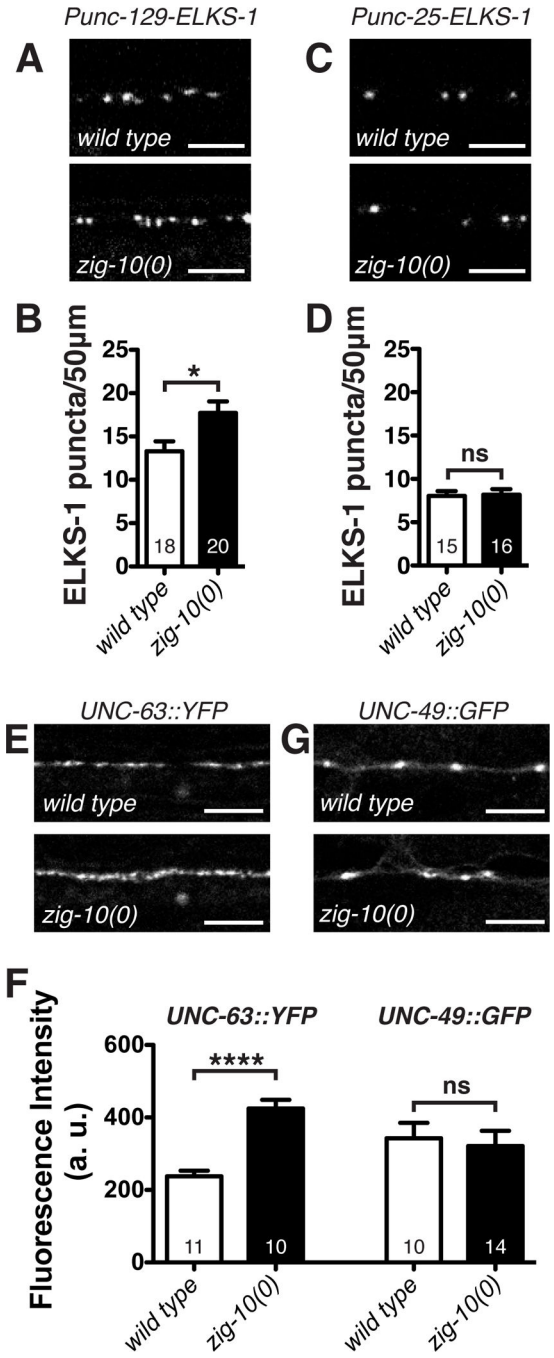

Figure 4. *zig-10* specifically regulates cholinergic synapse density

(**A**) Representative confocal images of adult animals expressing *Punc-129-ELKS-1::Cerulean (tauIs12)* in the cholinergic motor neurons. (**B**) *zig-10(0)* increased the density of cholinergic synapses. (**C**) Representative images of adult animals expressing *Punc-25-ELKS-1::tdTomato (nuIs249)* in the GABA motor neurons. (**D**) *zig-10(0)* animals displayed a normal density of GABAergic synapses. (**E**) Representative images of *UNC-63::YFP (kr98)* expressed from the endogenous locus (Gendrel et al., 2009). (**F**) *zig-10(0)* increased the intensity of cholinergic (UNC-63), but not GABAergic (UNC-49)

Author Manuscript Author Manuscript Author Manuscript Author Manuscript

postsynaptic receptors; data are presented in arbitrary units (a. u.). (**G**) Representative images of *UNC-49::GFP (oxIs22)* (Bamber et al., 1999).

Scale bars are 5 μm. The data in B, D, and F are represented as mean ± SEM. ns=not significant, *p<0.05, **p≤0.01, ***p≤0.001, and ****p≤0.0001. Sample size is shown within each bar. See also Figure S4.

Author Manuscript Author Manuscript Author Manuscript Author Manuscript

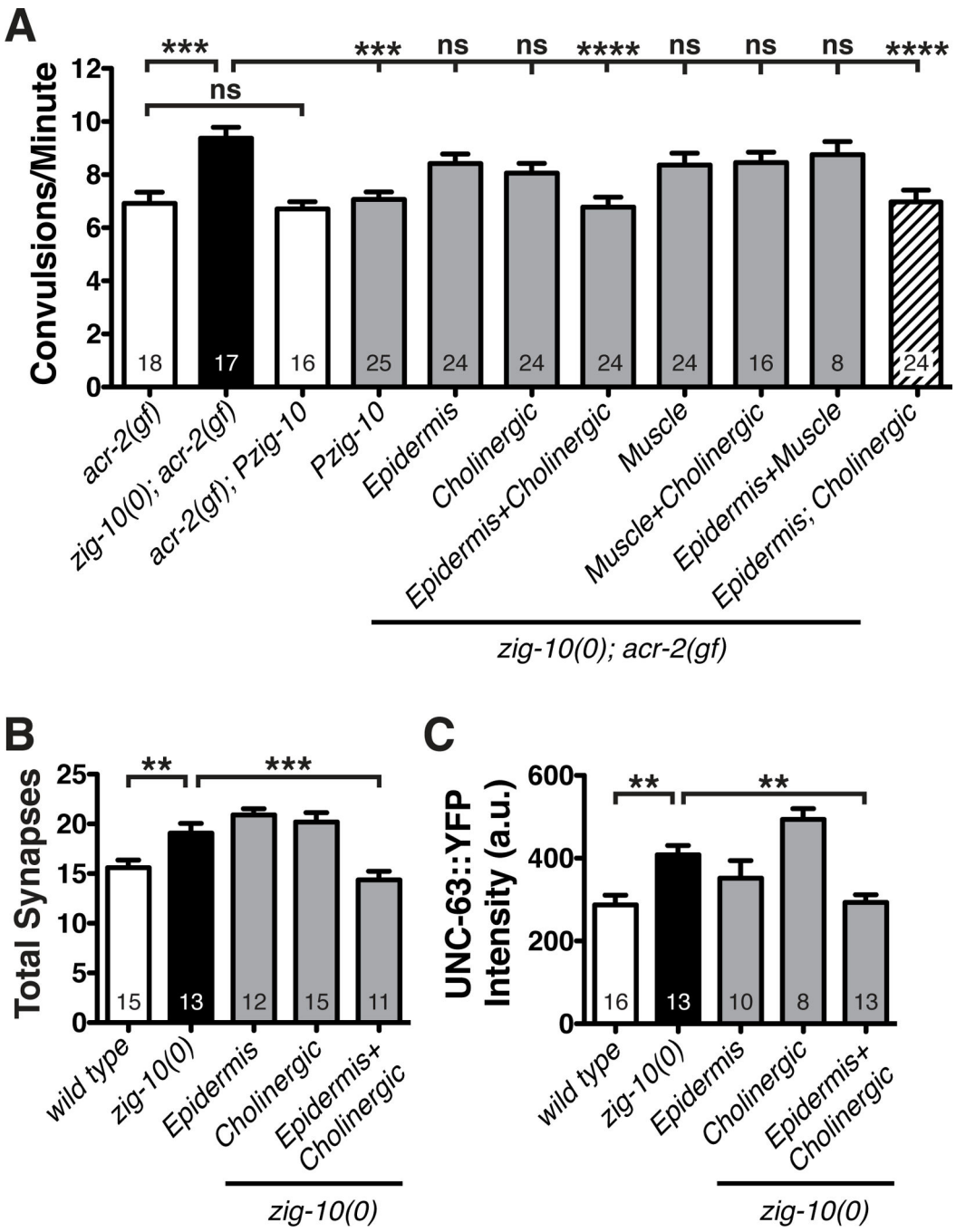

Figure 5. *zig-10* is required in the epidermis and neurons to modulate synapse density

(**A**) Simultaneous expression of ZIG-10 in cholinergic neurons (*Punc-17β*) and the adult epidermis (*Pcol-19*) reduces the convulsion frequency in *zig-10(0); acr-2(gf). Pmyo-3* was used for body wall muscles. Independent *Punc-17β-ZIG-10* and *Pcol-19-ZIG-10* transgenic animals were crossed to generate the strain in the striped bar. Additional independent transgenic lines for each promoter showed similar results as shown in the graph. See Table S2. (**B**) Simultaneous expression of cholinergic and epidermal ZIG-10 is sufficient to restore cholinergic synapse density (visualized by *Pmig-13-CFP::RAB-3 (wyIs109)* in DA9

Author Manuscript Author Manuscript Author Manuscript Author Manuscript

neurons). (**C**) Simultaneous expression of cholinergic and epidermal ZIG-10 is sufficient to reduce *UNC-63::YFP (kr98)* to wild type levels.

The data are represented as mean ± SEM. *p<0.05, **p≤0.01, and ***p≤0.001 and ****p≤0.0001. Sample size is indicated within each bar. See also Figure S5.

Author Manuscript Author Manuscript Author Manuscript Author Manuscript

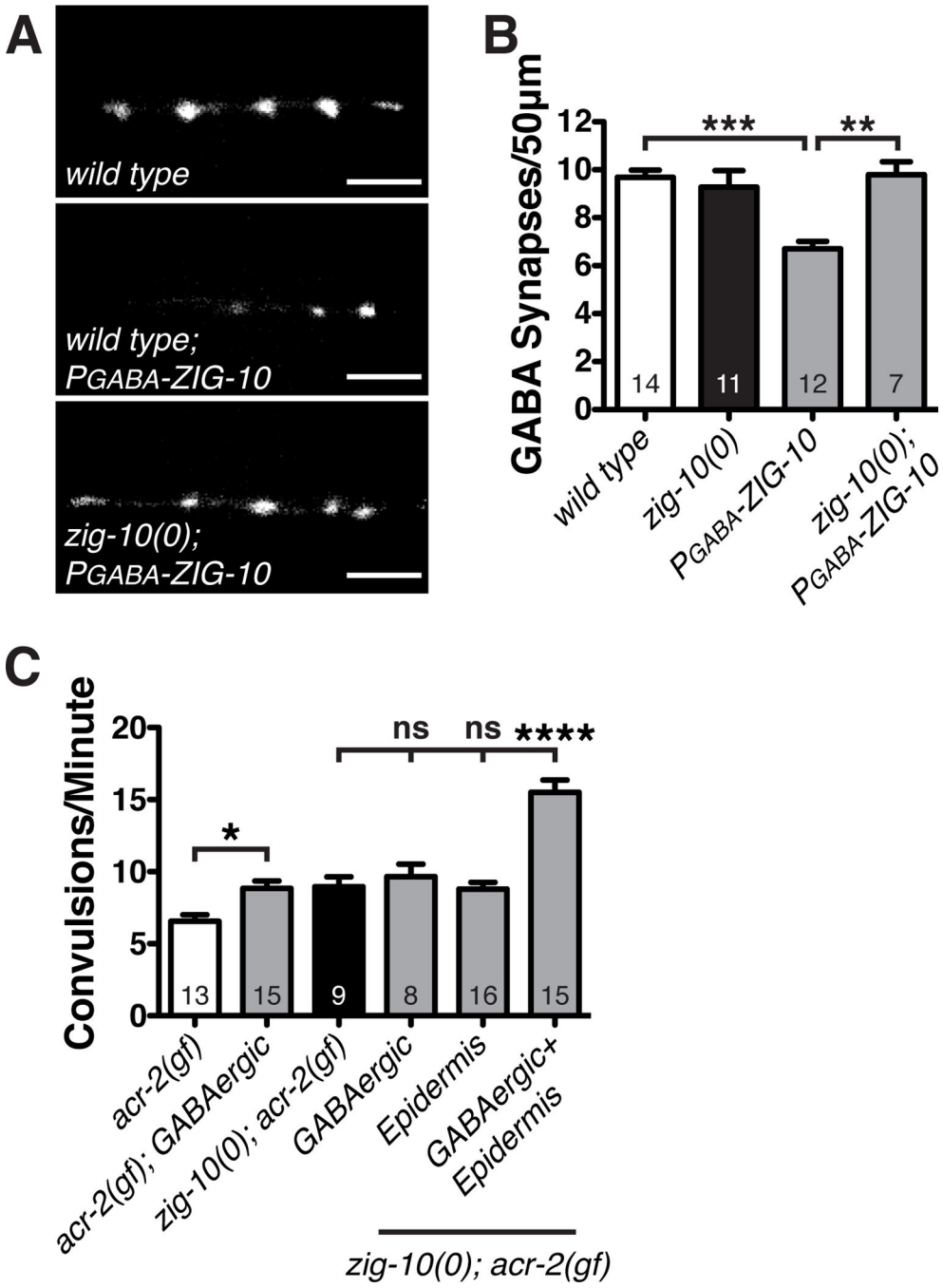

Figure 6. Ectopic ZIG-10 reduces GABAergic synapse density and exacerbates convulsion frequency of *acr-2(gf)*

(**A**) Representative images of *Punc-25-RAB-3::mCherry (juIs235)* in adult animals expressing P_{GABA}*-ZIG-10* in GABAergic neurons. Scale bars are 5 µm. (**B**) GABAergic expression of ZIG-10 in wild type, *not zig-10(0)*, reduces the density of GABAergic synapses. (**C**) Expression of ZIG-10 in GABAergic neurons enhances the convulsion frequency. The promoters used were: GABAergic neurons (*Punc-25*) and epidermis (*Pcol-19*).

Author Manuscript Author Manuscript Author Manuscript Author Manuscript

The data in B and C are represented as mean ± SEM. *p<0.05, **p≤0.01, and ***p≤0.001 and ****p≤0.0001. Sample size is indicated within each bar. See also Figure S6.

Author Manuscript Author Manuscript Author Manuscript Author Manuscript

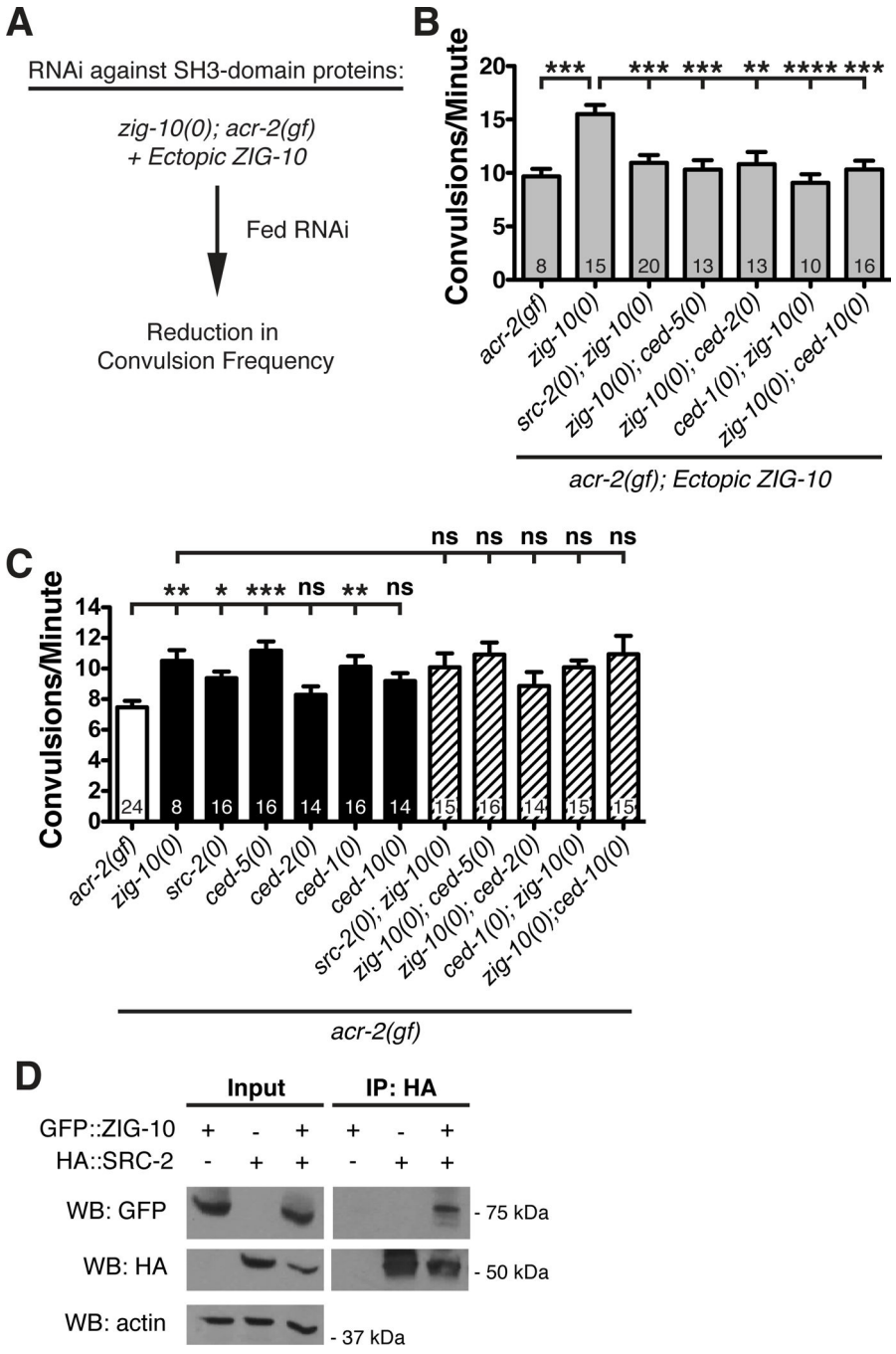

Figure 7. SRC-2 and the phagocytotic pathway act downstream of ZIG-10

(**A**) Schematic of the RNAi screen of SH3-containing proteins using the assay of enhanced convulsion frequency caused by ectopic ZIG-10 *[P_{GABA}-ZIG-10 + Pcol-19-ZIG-10*]. (**B**) *src-2(0), ced-5(0), ced-2(0), ced-1(0)*, and *ced-10(0)* reduced the convulsion frequency in *zig-10(0); acr-2(gf)* animals expressing ectopic ZIG-10 in both the GABAergic neurons and the epidermis. (**C**) *src-2(0), ced-5(0)*, and *ced-1(0)* increased the convulsion frequency in *acr-2(gf)* background. (**D**) ZIG-10 interacts with SRC-2 by co-immunoprecipitation.

Author Manuscript Author Manuscript Author Manuscript Author Manuscript

The data in B and C are represented as mean ± SEM. *p<0.05, **p≤0.01, ***p≤0.001, and ****p≤0.0001. Sample size is shown within each bar. See also Figure S7; Table S4.

Author Manuscript Author Manuscript Author Manuscript Author Manuscript

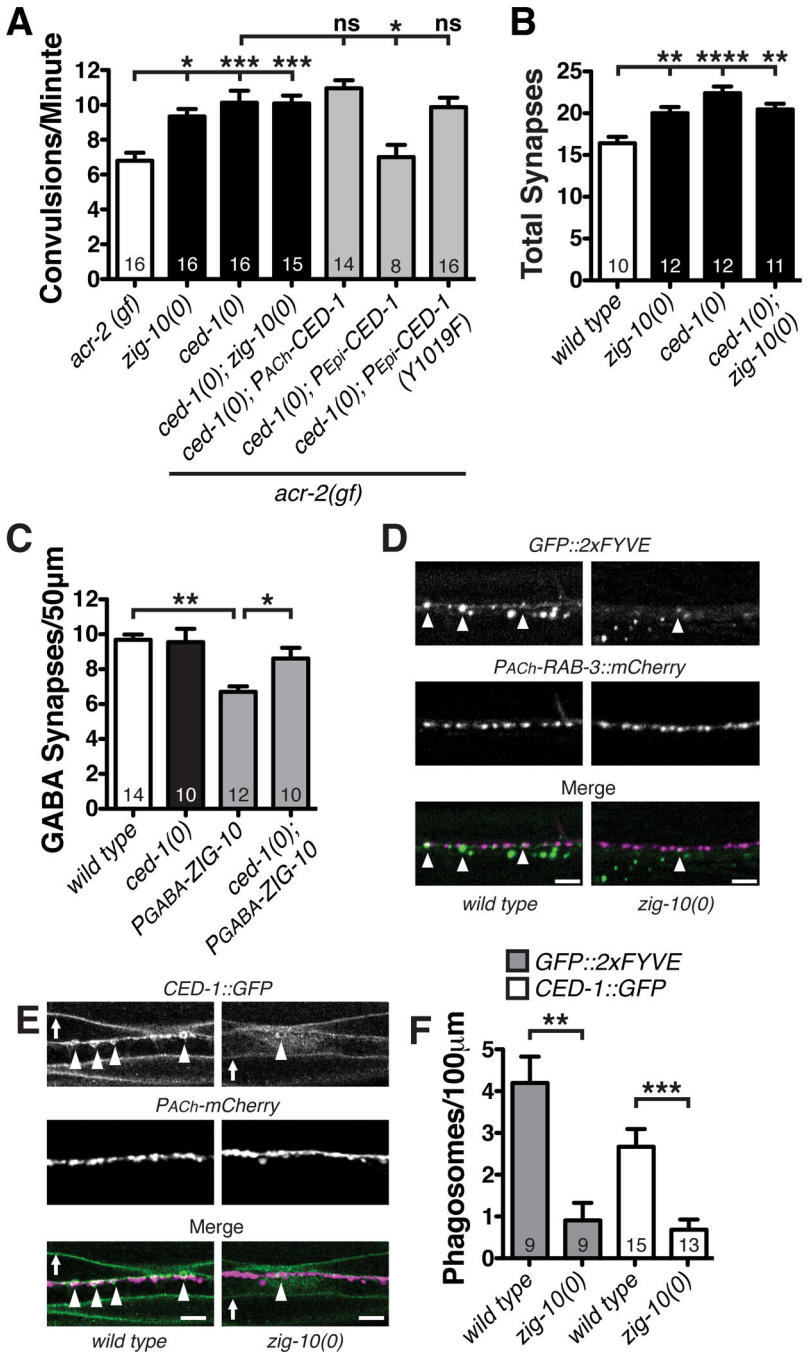

Figure 8. ZIG-10 regulates CED-1-mediated phagocytosis of synapses

(**A**) *ced-1(0)* increased the convulsion frequency in *acr-2(gf)* background. Wild type CED-1 expression in the epidermis, but not in cholinergic neurons fully restored the convulsion frequency. The nonphosphorylatable mutant CED-1(Y1019F) did not rescue *ced-1(0)*. (**B**) *ced-1(0)* showed increased number of cholinergic synapses (visualized by *Pmig-13-GFPSNB-1 (wyIs109)* in DA9 neurons). (**C**) *ced-1(0)* suppressed the reduction of GABAergic synapses in animals expressing P_{GABA}-*ZIG*- 10 (*juEx6246*). (**D**) GFP::2xFYVE under the ced-1 promoter was coexpressed with RAB-3::mCherry expressed under the *acr-2*

promoter. Arrowheads indicate GFP-2xFYVE colocalized with RAB-3::mCherry. (**E**) Representative images of CED-1::GFP coexpressed with mCherry driven by the *unc-17β* promoter. Arrowheads indicate CED-1::GFP-labeled phagosomes near the nerve cords; arrows denote CED-1::GFP on the muscle membrane. (**F**) *zig-10(0)* reduces the number of phagosomes labeled by GFP::2xFYVE or CED-1::GFP that colocalize with cholinergic neurons.

Scale bars are 5 μm. The data in A, B, C, and F are represented as mean ± SEM.*$p<0.05$, **$p\leq0.01$, ***$p\leq0.001$, and ****$p\leq0.0001$. Sample size is shown within each bar.

Author Manuscript Author Manuscript Author Manuscript Author Manuscript